Formation of graphene and hexagonal boron nitride on Rh(111) studied by in-situ scanning tunneling microscopy

Dong, G.

Chapter 8 Parameters influencing Graphene and Carbide formation

8.1 Introduction

The traditional parameters which are used to control the quality of graphene, formed by chemical vapor deposition (CVD), are gas pressure, substrate temperature, heating rate and cooling rate. In this chapter, ethylene deposition on Rh (111) is taken as an example. *In-situ* scanning tunneling microscopy (STM) measurements under various growth conditions and at temperatures up to 1100 K were performed, revealing the processes of graphene formation at the atomic level. We will start the discussion with the influence of the temperature on the formation of graphene and carbide. Then we will introduce a new degree of freedom, demonstrating that by separating the stages of nucleation and further growth and by controlling other growth parameters, we obtain graphene of higher quality, while avoiding carbide formation.

8.2 The temperature dependence of graphene and carbide formation

In order to obtain a first impression of the temperature dependence of graphene formation, we exposed the Rh surface to a high dose of ethylene at room temperature and slowly heated up the sample, while the surface was monitored continuously with STM. The initial, saturated layer of ethylene was obtained by exposing the freshly cleaned Rh(111) surface [73] in the UHV chamber to 3×10^{-5} mbar s of ethylene gas at room temperature. The result of this exposure is a pronounced, atomic-scale roughness,

decorating the entire surface (Fig. 8.1A), that we associate with the disordered overlayer of ethylene molecules. During the initial stages of the temperature ramp, clusters formed without any preference for specific edge orientations (Fig. 8.1B). These clusters grew in size when the temperature was increased. Even though we have directly observed the motion and coalescence of the clusters, the drifting during temperature changes makes is difficult to conclude that this was the sole ripening mechanism. Previous research showed ethylene decomposition on Rh to proceed in various stages at different temperatures up to ~800 K [61, 86]. Based on this, we interpret the irregular structures in Fig. 8.1B to be clusters of carbon or CH_x. At around 870 K, some islands were observed with a hexagonal shape, and the characteristic moiré pattern inside, indicating that, at this temperature, graphene had already been formed, and that the domains were large enough to appear as moiré patterns. The restructuring of the overlayer into graphene necessarily should start with small domains, smaller than one unit of the moiré pattern (2 x 12 x 12 carbon atoms). Ripening processes make some domains grow at the expense of others, to become larger than this size. Because any ripening process requires the relocation of many C atoms, this ripening should be relatively slow [87]. The combination of this slow ripening with the fast temperature ramp up to 870 K of 0.2 K/s, implies that the moiré pattern observed at 870 K is a sign that graphene formation had started already at a temperature below 870 K. Indeed, Fig. 8.1C shows our lowest-temperature observation of a moiré pattern, at 808 K, (temperature ramp rate was 0.05 K/s) close to the temperature range of 700-800 K, necessary for complete decomposition of ethylene [61, 86]. Up to 969 K, the ripening of the graphene islands continued, making the islands larger, more compact and more hexagonal (Fig. 8.1D). Also, the orientations of different domains became similar. Nevertheless, we still observed more than a single moiré pattern at this high temperature, which indicates that several overlayer orientations may have similarly low energies.

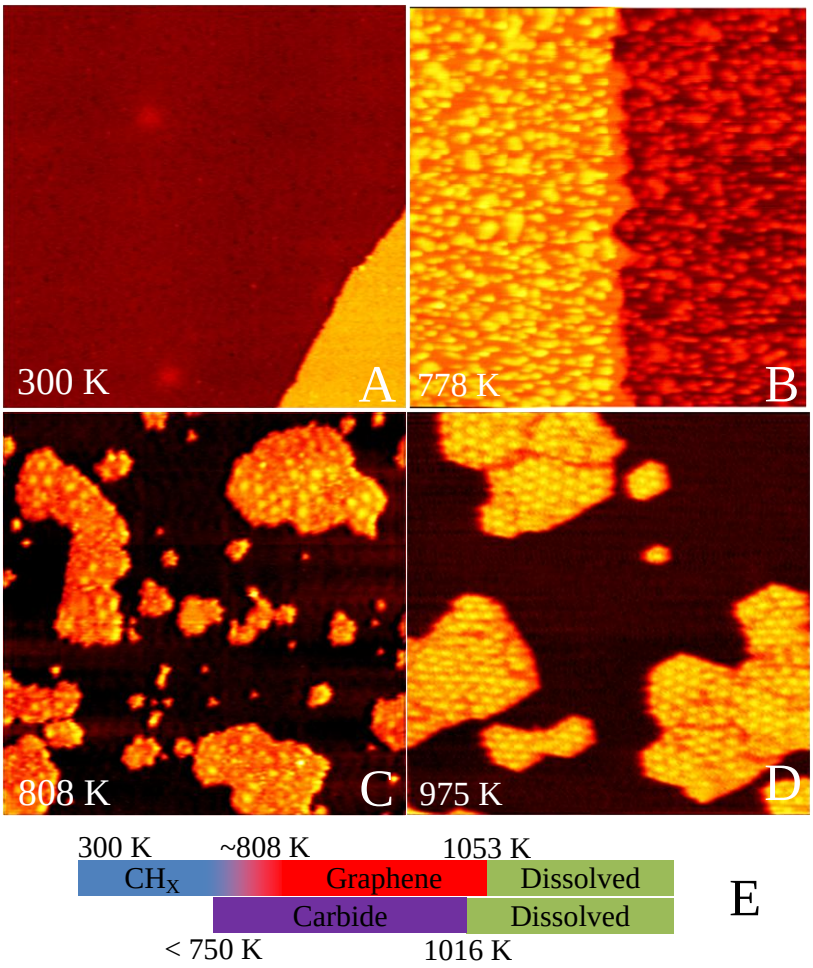

Fig. 8.1 STM images measured during continuous heating from 300 K to ~1000 K, after room temperature ethylene deposition. Panels A, B and D are from one series of experiments. (A) The Rh(111) surface directly after exposure to 3 x 10^{-5} mbar s of ethylene at room temperature. A mono-atomic step on the Rh surface crosses the image. The saturated ethylene adsorbed layer causes the rough appearance of the upper and lower terraces. (B) At 778 K, the overlayer organized into irregular clusters, but no moiré pattern was found at this temperature. (C) Starting from 4 x 10^{-7} mbar s ethylene exposure at room temperature, this image shows the lowest temperature where the moiré pattern of graphene was found. (D) At 975 K, the graphene had ripened into larger islands, with similar orientations. (E) Temperature ranges for the observed stability of graphene and carbide on Rh(111).
The STM images all have a size of 85 nm × 85 nm. They have been taken at sample voltages of V_b = 0.05 V, 1.16 V, 1.43 V, and -1.84 V for panels A, B, C and D, respectively, and at a tunnel current of I_t = 0.05 nA.

In a separate experiment we found that the graphene overlayer dissolved into the Rh substrate, starting at a temperature of ~1050 K. The information obtained from these heating experiments can be cast in the form of the upper temperature bar in Fig. 8.1E, displaying that, from 808 K to 1053 K, graphene can be formed on a Rh surface. This 250 K temperature range for stable graphene on Rh is much wider than the 50 K window that has been reported previously [88]. This process, combining adsorption of ethylene at room temperature with a subsequent temperature ramp, also yields a lower graphene formation temperature than the temperature of ~1100 K, reported in case ethylene was dosed directly at high temperature [89].

Similar to the case of *h*-BN nanomesh formation on Rh(111) [20], the quality of the graphene overlayer is limited by defects in the form of two different classes of domain boundaries. One class results from the merger of neighboring graphene islands with different orientations. On the atomic scale, this type of domain boundary must involve defects with respect to the hexagonal structure of perfect graphene, for example arrays of pentagons and/or heptagons [54] instead of the normal hexagons. The other class of domain boundaries originates from the merger of islands with precisely the same orientation. Due to the mismatch in lattice spacing between the overlayer and the substrate, there are still 288 translationally inequivalent possibilities to position the graphene on the Rh(111). This makes the probability for a perfect fit lower than 0.4%, so that most of these mergers will be accompanied by a phase defect line in the moiré pattern. Although such lines may look ‘dramatic’, we speculate that this phase defect is not leading to dangling bonds, i.e., the defect is present only in the period and the superstructure but not in the topology of the graphene network [54]. Since both classes of defects derive from the boundaries between individual graphene islands, the defect density is completely determined by the initial nucleation density of the growing overlayer.

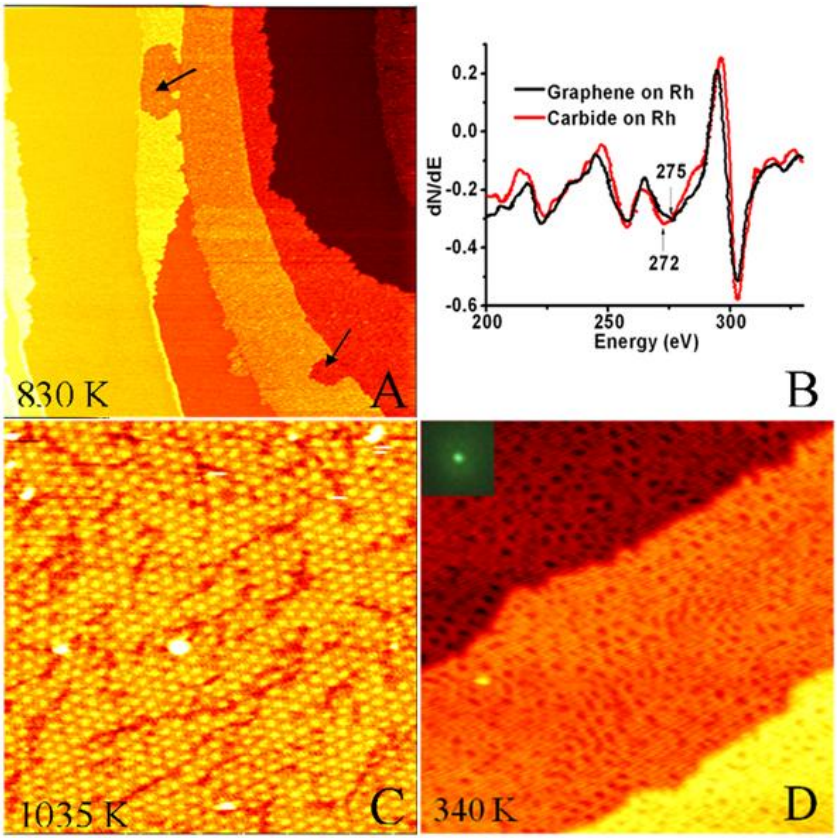

Fig. 8.2 Direct ethylene deposition at different temperatures. (A) An STM image measured at 830K, during deposition of ethylene. We interpret the rough layer that started to grow from the Rh steps as a carbide film (see text). Before nucleation of the film, the Rh steps were modified, as is indicated by the arrows. Nucleation started when the ethylene pressure reached 4.4 x 10^{-8} mbar. (B) Comparison between two Auger electron spectra of Rh(111); red: with a single-monolayer carbide covered Rh, formed by ethylene deposition at 750K, and black: with single-layer graphene. (C) A STM image of graphene-covered Rh, which was achieved by direct ethylene deposition at a pressure of 3.5 x 10^{-7} mbar and a temperature of 1035K. The image was taken at the growth temperature. The 'defect' lines in the image were formed already before the graphene overlayer nucleated. We associate these lines with dissolved carbon atoms. (D) STM image of the sample of (C), after it was cooled to 340 K. The moiré pattern of the graphene was deformed. The inset in (D) shows one integer-order Rh LEED spot (same view as in inset of fig. 1C) and the near absence of superstructure spots around it, recorded at room temperature.
The STM images all have a size of 85 nm × 85 nm. They have been taken at sample voltages of V_b = 2.79 V, 2.52 V, and 3.74 V for panels A, C, and D, respectively, and at a tunnel current of I_t = 0.05 nA.

In a first attempt to reduce the nucleation density, we increased the diffusion coefficient of adsorbed carbon atoms by exposing a clean Rh sample directly to ethylene at elevated temperatures, e.g. 750 K and 830 K. As predicted by nucleation theory [84], the high diffusion coefficient together with the low deposition rate should result in a lower nucleation density. With STM it was seen that an overlayer formed, starting from the steps on the Rh surface, and proceeding until it covered the entire surface. As can be seen in Fig. 8.2A, this overlayer had a structure that was different from that of graphene. After the entire surface had been covered by this layer, we heated the sample to higher temperatures, while monitoring the structure with the STM. It was found that the overlayer did not transform into the graphene structure even up to the temperature of 1016 K, at which it disappeared. The stability of the structure indicates that it did not consist of CHx clusters, which would otherwise have transformed into graphene at and above 808 K. We interpret the disappearance again as the dissolution of the deposited material into the Rh substrate. The fact that the dissolution temperature differs significantly from the value of 1050 K, mentioned above for graphene, indicates that in this case the overlayer was not graphene. Auger electron spectroscopy (AES) (Fig. 8.2 B) on this layer shows that the KLL of C peak had shifted from 272 eV to 275 eV and the MNN peak of Rh had also undergone a change in shape and position. Both shifts indicate the formation of a new compound [90]. We suggest that this is a rhodium carbide overlayer. Comparing this AES spectrum with a reference spectrum taken on a one-monolayer graphene-covered Rh surface (Fig. 8.2B), we see that the C-to-Rh peak ratios for these two cases were similar. Assuming that the Rh peak in the AES spectrum of graphene-covered Rh corresponds to effectively one atomic layer of Rh, we find that the C-to-Rh ratio in the carbide must have been in the order of 2:1. In analogy to the temperature bar for a graphene overlayer, the lower bar in Fig. 8.1E shows the growth and stability regime of a carbide layer on Rh(111).

Attempts were also made to deposite ethylene directly onto Rh, at an even higher temperature, still within the range where both graphene and carbide layers are stable (see the two bars in Fig. 8.1E), e.g. at 982 K. Here we observed regions similar to Fig. 8.2C and other regions similar to Fig. 8.2A, i.e. both graphene and carbide were present on the surface. Interestingly, there is a narrow temperature window, between 1016 K and 1053 K, in which a carbide layer is no longer stable, but a graphene monolayer is. In order to explore this window, we held the Rh at 1028 K, while dosing again with ethylene. Indeed, a graphene layer was observed to form at this temperature. It covered the entire

surface without a trace of carbide (Fig. 8.2C). However, the moiré pattern of the graphene overlaye became distorted during the slow cooling down, after the deposition, as shown in Fig. 8.2D. The low-energy electron diffraction (LEED) pattern that was taken afterwards at room temperature showed a weak Rh(111) pattern on a strong, diffuse background (inset Fig. 8.2D). We attribute the deterioration of the overlayer during the cooling down to segregation. it is known that carbon, which dissolves into the near-surface region of the Rh at the growth temperature, can segregate back to the surface when the temperature is decreased [73]. This segregation could lead to the nucleation of islands of a second graphene or carbide layer, between the original one and the Rh substrate, which will locally push up the graphene overlayer and distort it. We can exclude the alternative explanation that the deterioration of the graphene during cooling was caused by the differential expansion coefficient between graphene and the Rh substrate (in this temperature regime graphene has a negative expansion coefficient) [refs], since other experiments, in which the role of segregated carbon could be minimized (see below), showed that the quality of the graphene was not affected solely by large changes in temperature.

8.3 The crucial role of the history of the sample

The above experiments demonstrated that the temperature window for producing graphene by direct deposition is quite limited, and graphene formed in this temperature window distorts when the substrate is subsequently cooled to room temperature. On the other hand, the first experiment, which started with deposition at room temperature, showed a wider temperature window for graphene formation (upper bar in Fig. 8.1E), starting below and ending above the carbide window (lower bar in Fig. 8.1E). The lower onset temperature may be beneficial since it will eventually lead to a lower strain level in the graphene, once it is cooled down to room temperature, since there is a significant difference in thermal expansion between the graphene overlayer and the Rh substrate [91, 92]. The lower temperature is also helpful in reducing the level of carbon dissolution into the Rh substrate. The differences between the two experiments in Fig. 8.1 and Fig. 8.2A further suggest that the choice made by the growing overlayer between carbide and

graphene, in the temperature interval from 800 K to 1016 K, is fully determined by the structure of the early overlayer nuclei; in other words, graphene patches will continue to grow as graphene, whereas carbide patches will continue to grow as carbide. In turn, this suggests a refinement of our approach, namely to separate the stage of nucleation from that of further growth. For example, one could start with the graphene-seeded Rh surface from the first experiment, and expose that to further ethylene deposition under different conditions, in order to obtain full coverage by graphene. One may expect nucleation and growth of the graphene overlayer to follow well-known rules, in which the nucleation density is determined by F/D, where F is the flux of arriving atoms and D is their surface diffusion coefficient [84]. If the deposition is carried out very slowly, so that the number determined by F/D is smaller than the existing seed density on the surface, the newly arriving carbon atoms will all be incorporated onto the edges of growing graphene islands, thus preventing them from forming new nuclei [93]. The presence of the graphene seeds on the surface should have the additional effect that newly arriving carbon atoms have a strongly reduced probability to dissolve into the Rh, again because they will be incorporated in the graphene overlayer on a much shorter timescale, due to the difference in the rates of diffusion of the carbon atoms into the bulk and over the surface, which should be expected to be significant. On a non-seeded surface, dissolution has to compete only with the rather rare processes of nucleation of either graphene or of carbide. How 'difficult' graphene nucleation is on a hot Rh surface is evidenced by our findings in a separate experiment, on a clean Rh surface: at 1028 K, an ethylene pressure of to 3.5×10^{-7} mbar was required to observe the first graphene nuclei in our STM images.

The suggested approach, of ethylene deposition at high temperatures onto a Rh surface that has been pre-seeded with graphene by low-temperature deposition, was successful. Fig. 8.3 shows the result obtained at a growth temperature of 975 K; even more informative is the corresponding STM movie, which can be found online. Starting with the end situation of the first experiment (Fig. 8.1D), ethylene was deposited, at a pressure of 3×10^{-9} mbar, which was increased at the end of the procedure to 1×10^{-8} mbar, simply to accelerate the process. The newly arrived carbon atoms continued with the structure and orientation of the graphene that was already present, until the entire surface was covered by graphene. When a new kink formed at a concave corner between two differently oriented domains, it showed a preference for following the graphene domain which had the same, or a similar orientation, as the Rh crystal. In this way, the metal

substrate guided the orientation of the graphene layer, and the density of domain boundaries became lower than that expected from the initial configuration of the graphene seeds. After this sample had been cooled down to room temperature, neither STM nor LEED (insert of Fig. 8.3B) showed a deformation of the moiré pattern. The LEED pattern showed that the graphene layer had a preferred orientation; otherwise, a ring of intensity should have been observed around the integer-order maxima from the Rh, rather than the six superstructure spots that are clearly present in the LEED pattern. Although the superstructure spots are not very sharp, the orientation difference between graphene domains is seen to be minor, because the moiré pattern is an amplifier of all variations in position and orientation. The bright regions, indicated by black arrows in Fig. 8.3B, were formed in the final stage of the deposition. They will be explained in Chapter 10.

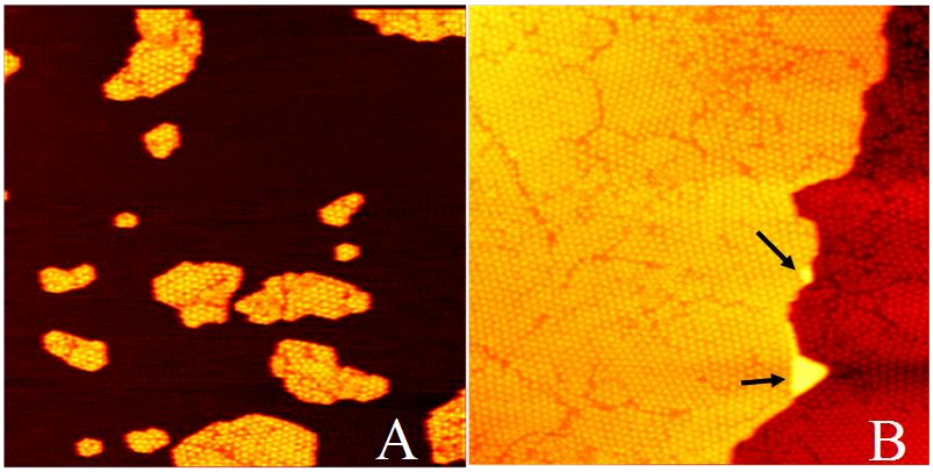

Fig. 8.3 STM images of graphene formation, starting with a seeded surface. (A) The graphene-seeded Rh surface achieved by annealing a pre-deposited sample from room temperature to 975 K. Most of the graphene islands had same orientation. But superstructure domain boundaries can be found within individual islands. (B) Graphene-covered Rh, after ethylene deposition at 975K on the seeded surface, at pressures ranging from 3×10^{-9} to 1×10^{-8} mbar over a period of 76 minutes. During this procedure, The domain boundary density became ~30% lower than that in the starting situation. (A). Two Rh double-layer defects are indicated by the arrows. The inset in (B) shows the superstructure spots around one Rh LEED spot.
All images are 160 nm × 160 nm and have been taken at a sample voltage of V_b = -1.84 V and a tunneling current of I_t = 0.05 nA.

8.4 Conclusion

In this chapter we have measured the formation and dissolution temperatures for both graphene and carbide. Although graphene can be formed at 800 K by ethylene exposure at room temperature and annealing, direct exposure of ethylene of the Rh surface at 800 K – 1000 K results in carbide formation. Ethylene exposure of Rh at 1035 K provided a graphene layer at high temperature, but the moiré structure was distorted during cooling of the sample. To solve these problems, a new element was introduced, which is the initial nucleation stage. It determines nearly completely the phase in which further C is incorporated, graphene or rhodium carbide, and it determines the variation in orientation of the growing graphene patches. We demonstrate that by separating the stages of nucleation and further growth and by controlling other growth parameters, we obtain graphene of higher quality, while avoiding carbide formation and controlling the dissolving of C.